RESEARCH ARTICLE

INTERNATIONAL RESEARCH JOURNAL OF MULTIDISCIPLINARY TECHNOVATION

Asian Research Association

DOI: 10.54392/irjmt25514

Deep Learning Based Detection and Classification of Gastrointestinal Abnormalities from Endoscopic Imaging Data

T. Swetha Kumari [a,*], R. Vasuki [a]

[a] Department of Biomedical Engineering, Bharath Institute of Higher Education and Research, Chennai - 600 073, India.
* Corresponding Author Email: swetha837@gmail.com
DOI: https://doi.org/10.54392/irjmt25514
Received: 25-06-2025; Revised: 14-09-2025; Accepted: 21-09-2025; Published: 30-09-2025

Abstract: Gastrointestinal (GI) abnormalities, such as polyps and ulcers, detected through endoscopic imaging are critical for diagnosing severe conditions like colorectal cancer. Accurate detection requires handling challenges such as subtle abnormalities and imbalanced datasets. Traditional detection methods often face difficulties in optimizing model parameters, segmenting abnormalities accurately, and maintaining a balance between speed and precision. The objective is to develop an efficient and robust hybrid technique, Dynamic vortex search-tuned Customized You Only Look Once version 8 (DVS-CYOLOv8), for enhanced detection and classification of GI abnormalities, DVS is utilized for optimizing hyper parameters such as anchor boxes and confidence thresholds while also identifying critical regions of interest. CYOLOv8 leverages advanced segmentation and multi-scale feature detection for real-time performance. A benchmark dataset of annotated endoscopic images covering a range of GI abnormalities is utilized. Preprocessing includes Median Filtering and Contrast Limited Adaptive Histogram Equalization (CLAHE) to suppress noise and improve contrast. Gradient-based techniques are applied for texture and boundary feature extraction. CYOLOv8 captures abnormalities and segments their boundaries with precision, adapting to abnormalities of varying sizes through its multi-scale architecture. DVS optimizes model configuration and enhances sensitivity by focusing on key regions, reducing false positives. It achieves exceptional accuracy (99.11%), precision (98.24%), recall (98.18%), and F1-score (97.66%), outperforming standalone techniques. That presents a scalable and effective clarification for GI abnormality detection, leading to enhanced clinical diagnostics.

Keywords: GI abnormalities, Endoscopic imaging, Medical images data, Dynamic vortex search-tuned Customized YOLOv8 (DVS-CYOLOv8 arch).

1. Introduction

Gastrointestinal (GI) abnormalities refer to any condition that affects the digestive system. The most frequent GI illnesses are polyps, infections, cancer, ulcerative colitis, and diverticulitis, among others. The World Health Organization (WHO) ranks these disorders among the top ten reasons for mortality in humans [1] the main cause for this enormous number of deaths is a lack of understanding regarding illness categorization using endoscopic imaging. GI endoscopy is becoming a widely utilized procedure for diagnosing and managing GI tract disorders. An endoscope is flexible tubing with a camera that passes via the patient's mouth or rectum and navigates through the patient's intestines [2]. The gastroenterologist can examine an image of the GI tract on a screen and physically identify and categorize anomalies in real-time. The gastroenterologist is responsible for endoscopic evaluation and illness categorization decisions. In this regard, the results can vary from one doctor to another. Thus, correct illness categorization is important since it influences therapy planning and follow-up of patients [3]. The current illness evaluation method has to be improved further to enhance the quality of GI tract diagnosis and therapy. Therefore, an autonomous recognition and categorization system would likely be effective in optimizing the current approach. The assessment of complaints and therapy commencement should be more reliable and efficient. Both regular and unusual results must be noted in documentation for further examination of patients. Because of all of these factors, a self-sufficient system could offer an affordable option by reducing clinician burden and information while enhancing illness detection uniformity, productivity, and time spent on patient care. Furthermore, an early diagnosis of the condition could help in controlling infections or prevention [4]. There are currently various ways to investigate illnesses in the GI tract, the most common of which is doctor-evaluated diagnostic imaging and testing in the lab. However, the illness's severity could vary considerably amongst specialists [5]. A fast

and precise diagnosis marks the beginning of proper therapy. Scientific research has made significant improvements to health, including image processing, large data leadership, and Artificial Intelligence (AI). Advanced imaging methods have enabled the visualization of hitherto inaccessible areas of the human body. Endoscopy is a type of these techniques; it is commonly used to inspect the GI tract by inserting a tube containing a camera within it [6]. Consequently, endoscopic examination of disease classification highly relies on the choice that gastroenterologists make, meaning that it can be different even doctor to doctor. Prolonged processing of endoscopic data and high levels of concentration are required, taking place manually, and sometimes may be inaccurate, depending on the inexperience of doctors. Consequently, automatic recognition might be beneficial in streamlining this process in the dimensions of time, cost, and the output in terms of categorization quality [7]. The most recent trend in terms of addressing medical imaging problems is the DL-based solutions with said technology being considered the most highly preferred method of addressing medical imaging problems. The performance of Deep Learning (DL) has significantly surpassed the conventional Machine learning (ML) methods due to the increased speed in processing power on Graphics Processing Unit (GPU) [8].

Despite these breakthroughs, there is still a need to establish more robust diagnostic AI tools GI abnormalities; the main limiting factor is access to large-scale, high-quality annotated datasets, and the process of labeling of such medical imaging data is labor-intensive and costly [9]. It is therefore of great importance to ensure that DL models are generalizable to most human populations of patients, imaging types and clinical settings when planning to use them in the real world [10]. Solving these issues will require a multidisciplinary approach, combining the talents of gastroenterologists, computer scientists, and biomedical engineers to create AI-based solutions aligned with the needs of the clinic [11]. The application of DL in endoscopic imaging holds great promise for making a radical change in the diagnosis of GI diseases through better diagnostic accuracy, lower diagnostic workload, and real-time decision support. As research in this area goes on, a combination of AI with endoscopy is expected to become part and parcel of practice, enhancing the early detection and treatment of GI disorders [12].

1.1 Aim

This research proposes the Dynamic vortex search-tuned Customized You Only Look Once version 8 (DVS-CYOLOv8) framework for enhanced detection and classification of GI abnormalities in endoscopic images. The primary focus is to reduce computational complexity, improve detection accuracy, and optimize real-time performance. Using the DVS optimization, the approach, on the contrary, dynamically tunes hyper parameters to obtain better performance in the field of medical imaging. The research seeks to bridge the gaps between issues of misclassification, processing efficiency, and real-time adaptability in the detection of GI diseases.

1.2 Research Gap

The GI abnormality detection field using DL is indeed full of challenges. Manual endoscopic evaluation and classical ML models succumb to inconsistencies in the grading of GI disorders due to inter-observer variability amongst gastroenterologists. The subjective view of the disorders can lead to misclassification, which is vital to the treatment outcome. In addition, manual analysis is slow and requires expertise, as it is prone to errors. Its inefficiency restricts its utilization in large-scale clinical applications. Even if DL-driven advancements have shown promise, many of those existing models took a hit on generalization, affecting patient populations and imaging modalities. These were all a result of the absence of a large volume of high-quality, annotated datasets, wherein expert labeling is time-consuming and costly. DL models typically require a great deal of power, which severely limits their application in resource-constrained clinical environments. Currently, YOLO-based models have great efficiency in detecting objects but lack specialized optimization strategies for medical imaging, limiting their feature extraction and localization accuracy. To bridge these gaps, the present research proposes DVS-CYOLOv8, putting to use hyperparameter tuning and real-time adaptability or adjustment to boost detection accuracy, computational efficiency, and possible applicability in clinical practice. This research therefore proposes an optimal solution of automated GI abnormality classification, which will reduce the workload and enhance early disease detection. The remaining section of this research is organized in the following manner: Section two depicts the literature surveys; In Section three, the proposed approach is described. In Section four, the results are explained. Section five presents thorough discussions of the results, prior to concluding the research in Section six.

2. Related work

Investigations of literature surveys on GI abnormality detection and classification from endoscopic images are summarized in Table 1.

3. Research Methodology

The dataset serves as the basis for the detection and classification of GI abnormalities. The image quality is enhanced by preprocessing with a Median Filter and Contrast Limited Adaptive Histogram Equalization.

Table 1. Analysis of Prior Studies in Gastrointestinal Abnormalities

Reference	Objective	Method	Limitation	Findings
[13]	To develop a Deep Convolutional Neural Network (DCNN)-based method for medicinal image processing, mainly for endoscopic image analysis, to identify GI problems.	Utilized multiple pathways, image resolutions, and convolutional layers in a DCNN model to assist gastroenterologists in detecting GI tract anomalies.	The research does not account for real-time clinical deployment challenges, such as variability in image quality and patient conditions.	The proposed model outperforms existing techniques, demonstrating its potential to enhance GI disorder classification by standardizing detection processes.
[14]	To explore the effectiveness of color and Texture Enhancement Imaging (TXI) and Red Dichromatic Imaging (RDI) in detecting Upper Gastrointestinal (UGI) disorders.	TXI was applied to improve texture, luminosity, and color tone for better disorder identification, while RDI was used to locate bleeding sites in endoscopic procedures.	The research lacks large-scale validation studies and does not explore the applicability of these techniques across different patient demographics.	TXI enhances visualization of UGI disorders, while RDI aids in pinpointing bleeding sites during endoscopic examinations.
[15]	To evaluate neural network architectures used in radiography, endoscopy, and histology for diagnosing GI disorders.	Applied DL techniques for lesion detection and characterization in endoscopic images.	The research does not assess real-world clinical implementation and fails to address computational resource limitations in hospitals.	AI-based DL techniques improve diagnostic accuracy and medical decision-making in GI disorder assessments.
[16]	To develop an AI-based system for GI disease diagnosis using Convolutional Neural Networks (CNNs).	Compared different CNN architectures with Residual Network-50 (ResNet50).	Limited dataset size restricts generalizability, and real-time implementation challenges are not discussed.	ResNet50 beats other methods in terms of accuracy and robustness for diagnosing GI diseases.
[17]	To introduce a novel dataset of Esophagogastroduodenoscopy (EGD) images for classification and to improve diagnostic effectiveness.	Developed a DL-based classification model that compares predicted labels with actual diagnoses.	The dataset is limited in diversity, which could affect generalizability across different patient populations.	DL-based classification significantly enhances the efficiency and accuracy of endoscopic image interpretation.
[18]	To assess AI's role in diagnosing upper GI	Applied AI-driven techniques for	Limited by small sample sizes and	AI aids in early cancer detection

	malignancies using white-light endoscopic imaging.	tumor detection in endoscopic images.	a lack of large-scale datasets for stomach cancer research.	but requires larger datasets for more reliable performance.
[19]	To analyze how AI improves diagnostic accuracy and efficiency in GI endoscopy.	Implemented DL models to enhance endoscope quality and reduce missed assessments.	Image variability and lack of large-scale randomized research remain challenges.	AI improves assessment accuracy but requires further validation through multicenter researches.
[20]	To develop an automated diagnostic system for GI disorders using deep CNN with cosine similarity feature selection.	Utilized a minimal deep CNN algorithm with feature reduction via cosine similarity.	The research does not evaluate the model in real-world hospital settings.	The proposed system achieves 97.68% accuracy, demonstrating reliability in healthcare diagnostics.
[21]	To enhance GI disorder diagnosis using traditional image processing and a preconditioned deep CNN.	Used VGG16 for classification.	The dataset lacks diversity, limiting model generalizability.	VGG16 outperforms other architectures with 96.33% accuracy.
[22]	To explore AI applications in colorectal polyp detection, stomach cancer diagnosis, and Wireless Capsule Endoscopy (WCE).	Applied DL-based CNNs for various GI applications.	The research does not consider real-time deployment challenges in clinical settings.	AI significantly enhances diagnostic accuracy in GI endoscopy.
[23]	To develop an endoscopy image classification model for diagnosing GI conditions.	Implemented a CNN-based model.	Does not address model performance on unseen real-world data.	CNN achieves in recall and accuracy (97.99%).
[24]	To improve lesion detection in endoscopy using Multi-Scale Context-Guided Deep Networks (MCNet).	Developed MCNet to capture local and global image features for improved classification.	Requires more computational resources, making real-time deployment challenging.	MCNet enhances lesion classification performance in endoscopic images.
[25]	To establish clinical 3D printing standards for diagnosing GI, hepatobiliary, and colorectal disorders.	Developed strategy according to the radiological society of North America's special interest group on 3d imaging.	The recommendations lack experimental validation in clinical settings.	The research provides a framework for clinical 3D printing applications in diagnosing GI diseases.
[26]	To integrate DL-based classification networks for GI disorder diagnosis.	Combined classification networks with a retrieval system.	The model's performance in rare conditions is not evaluated.	The approach outperforms conventional methods in

				accuracy, aiding early detection and treatment.
[27]	To develop Transmission Network (TransMT-Net) for improved lesion detection in endoscopic images.	Integrated CNN's local and global features into a multi-task system.	Requires further validation on larger datasets.	The model effectively detects lesions, enhancing diagnostic efficiency and achieving 96.94% accuracy.
[28]	To address limitations in Wireless Capsule Endoscopy (WCE), this image datasets used a Wireless Capsule Endoscopy-Deep Convolutional Generative Adversarial Networks (DCGAN) WCE-DCGAN system.	Used DCGAN for synthetic WCE image generation.	Model effectiveness is restricted by dataset biases.	The system improves WCE image-based disorder detection accuracy (97.25%).
[29]	To evaluate DL models for GI disorder diagnosis.	Compared GoogleNet, ResNet-50, and AlexNet for endoscopic image classification.	The research does not examine model robustness under varying lighting and noise conditions.	AlexNet achieves superior diagnostic accuracy compared to other models.
[30]	To develop a segmentation and classification model for GI diseases using WCE images.	Combined improved U-Net with an enhanced Deep Neural Network (DNN) for better segmentation.	The research does not evaluate real-world deployment challenges.	The proposed method surpasses baseline approaches in classification performance.

(CLAHE). Feature extraction takes place via the Gray Level Co-Occurrence Matrix (GLCM), providing features based on the images' texture properties. Coupled with the above, the DVS-CYOLOv8 does the heavy lifting of GI abnormality detection and classification from endoscopic images, ensuring improved localization and recognition accuracy. Research flow is represented in Figure 1.

3.1 Data Collection

This research employs the Kvasir Dataset for Classification and Segmentation, an open-access [31] multi-class image data for the recognition of GI diseases.

These are high-resolution endoscopic images that cover three anatomical landmarks, three pathological outcome classes, and two endoscopic procedure-related classes. Kvasir contains Class 0 Normal-Pylorus, Class 1 Polyps, Class 2 Ulcerative Colitis, and Class 3 Esophagitis, so it covers almost all evaluations of GI abnormalities. The data set supports image classification, segmentation, and retrieval tasks and is thus appropriate for DL and transfer learning uses. Likewise, the Kvasir Polyp Segmentation (Kvasir-SEG) subset includes 1,000 polyp images with associated segmentation masks that can allow accurate lesion detection.

3.2 Preprocessing Using Median Filter And Contrast Limited Adaptive Histogram Equalization (CLAHE)

To eliminate salt and pepper noise, a 3D median filter is used for the collected data. The procedure is outlined in Equations (1)-(3).

$$\zeta_B(j,i) = \sum(\zeta_s(j,i), I(j,i)) \quad (1)$$

$$\zeta_D(j,i) = \sum(\zeta_C(j,i), \zeta_a(j,i)) \quad (2)$$

$$\zeta_N(j,i) = E_{MD}(\zeta_D(j,i), b) \quad (3)$$

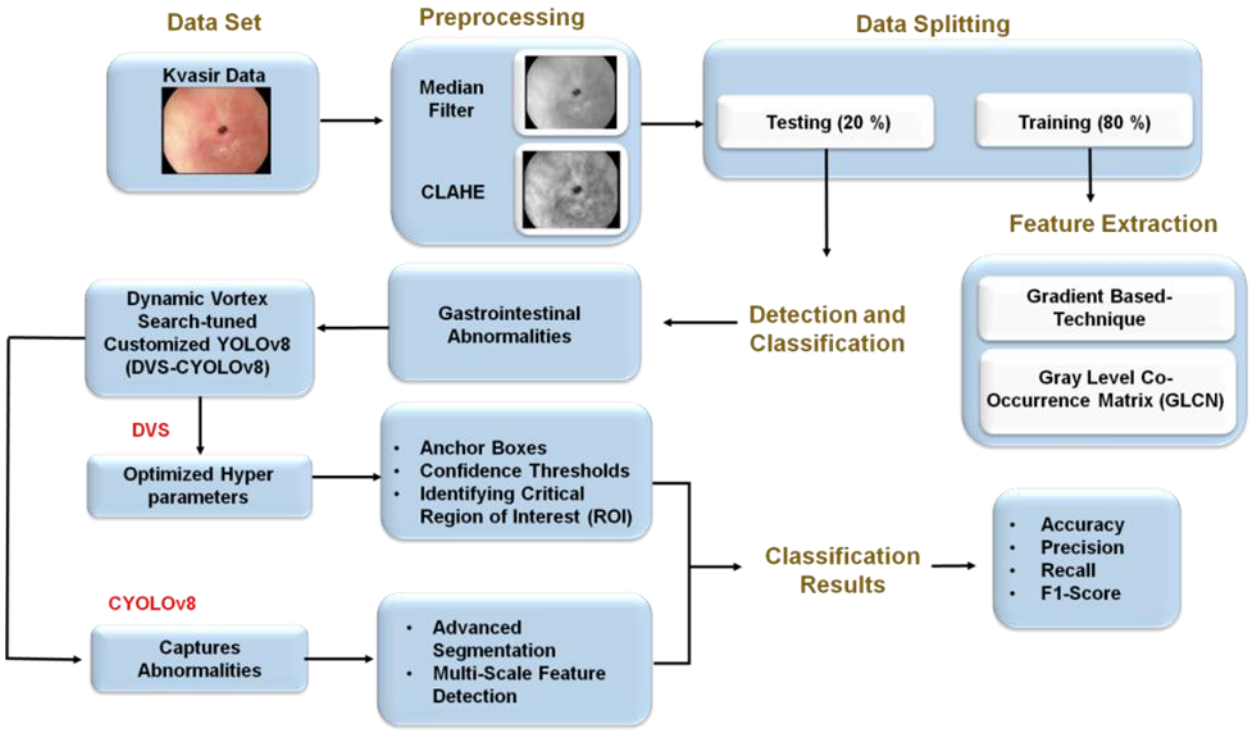

Figure 1. Working principle of proposed methodology

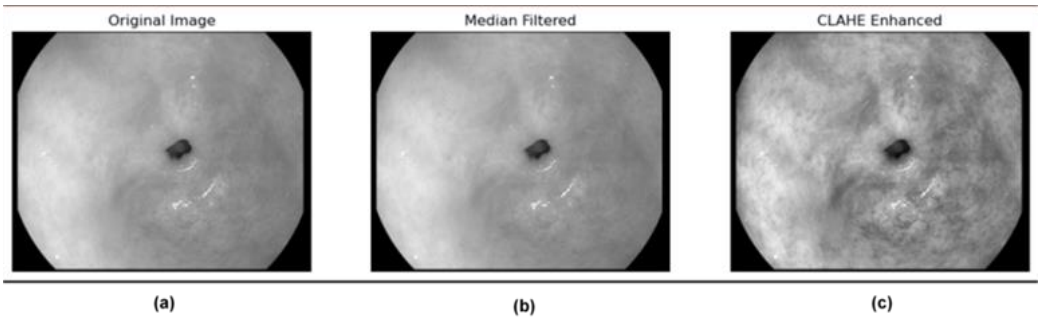

Figure 2. Preprocessed images (a) Original Image, (b) Median Filter, and (c) CLAHE-enhanced

Where $\zeta_B(j,i)$ indicates the sum of the top-hat and initial pixels, $\zeta_D(j,i)$ indicates the integrated pixels data image, $\zeta_N(j,i)$ indicates the 3D median filtered image, E_{MD} indicates the median filtered operation, and α indicates the filter dimension (3 × 3 × 3).

CLAHE is an image enhancement approach that utilizes a histogram equalization approach. CLAHE addresses the issue of excessive contrasts by offering an edge value for the histogram. The clip limitation indicates the greatest height of a histogram. Equation (4) defines how to compute the visual limits of a histogram

$$\beta = \frac{N}{M}\left(1 + \frac{\alpha}{100}(T_{max} - 1)\right) \quad (4)$$

The variables M (area size), N (grayscale value of 256), and α (clip component) represent the insertion of a histogram ranging from 0 to 100. The CLAHE process begins with determining the area's size and clip limitation, followed by shaping the histogram for every area, distributing over clip minimize values, mapping the updated histogram to the image, and interpolating pixels in nearby regions to produce the finalized CLAHE image. Figure 2 depicts the preprocessed images using a (a) original image, (b) median filter and (c) CLAHE.

3.3 Feature Extraction Using Gray Level Co-Occurrence Matrix (GLCM)

The closest neighbor interpolated approach was employed to alter the image dimensions of pulmonary nodules Region of Interests (ROIs) taken from the initial image. This ensured that all ROIs remained the same size. The image is then up-sampled to increase its gradient data. Then, every image is segmented into 2x2 sub graphs to obtain the intrinsic gradient data more evenly.

3.3.1 Identifying Gradients

The histogram of oriented gradients (HOG) feature generator counts gradient directions in the

specific target area of an image to reflect the area's model and shape. Gradient data represents the edge, contour, shape, and additional textural properties of the items in the image. Most lung nodules have distinct interior textures and clear boundaries. The HOG characteristic could identify gradient data in ROI regions of pulmonary nodules, allowing for the extraction of GLCM texture features using sliding window adaptive techniques.

The particular stages are as follows.

Step 1: Involves preprocessing the image and standardizing it with the Gamma correction technique to improve contrast and reduce noise.

Step 2: Split the image into contiguous sections (cell units) and gather gradient direction values for every pixel. To calculate the path of a gradient measurement for each pixel point, the image's horizontal and vertical dimensions are used as input.

In the experiment, the image's gradient and orientation were calculated using the model [-1, 0, 1]. The gradient generator calculates the gradient in both vertical and horizontal orientations. The image's pixel location was determined at (w, z), and a gradient was calculated using the following Equation (5)

$$\begin{cases} H_w(w,z) = G(w+1.z) - G(w-1,z) \\ H_z(w,z) = G(w,z+1) - G(w,z-1) \end{cases} \quad (5)$$

The equation uses $H_w(w,z)$, and $H_z(w,z)$ to convey the horizontal and vertical gradients at each pixel position (w,z) in the input image. Equations (6) and (7) provide the magnitude $H(w,z)$, and gradients $\alpha(\mathrm{w},\mathrm{z})$ orientation equations for the pixel position (w,z).

$$H(w,z) = \sqrt{H_w(w,z)^2 + H_z(w,z)^2} \quad (6)$$

$$\alpha(\mathrm{w},\mathrm{z}) = \tan^{-1}\left(\frac{H_w(w,z)}{H_z(w,z)}\right) \quad (7)$$

Step 3: Determine the intensity and gradient directions of each pixel point, then identify gradients at zero-crossing places in the image, including the zero-crossing location of $H(w,z)$. GLCM feature values are shown in Figure 3.

3.4 Detection and Classification Of GI Abnormalities Through Endoscopic Images Using Dynamic Vortex Search-Tuned Customized Yolov8 (DVS-Cyolov8)

To develop a hybrid DVS-CYOLOv8 technique that is robust and efficient in its enhanced detection and classification of GI abnormality. The DVS algorithm is used to optimize hyperparameters such as anchor boxes confident thresholds and also the identification of important areas of interest. CYOLOv8 exploits advanced segmentation and multi-scale feature detection for real-time performance.

3.4.1 Customized YOLOv8 (CYOLOv8)

The proposed DVS-CYOLOv8 model integrates GLCM-based feature extraction to enhance GI abnormality detection in endoscopic images. Key GLCM features such as contrase, dissimilarity, homogeneity, energy, and correlation aid in distinguishing abnormal tissues (Figure 3). Combined with CLAHE, median filtering, and gradient-based technique, the model achieves high accuracy and robust segmentation for improved clinical diagnostics. CYOLOv8 is customized a YOLO-based architecture (Figure 4) designed for detecting and classifying GI abnormalities in endoscopic images with enhanced accuracy and efficiency. The model employs Convolution + Batch Normalization + Rectified Linear Unit (COnvBNReLU) blocks for initial feature extraction, followed by Decoupled Depthwise expansion (D2e) modules that enhance deep feature learning. It integrates Simple Spatial Pyramid Pooling-Fast (SimSPPF) for spatial pyramid pooling and Large Selective Kernel (LSK) attention to capture long-range dependencies, improving detection performance. The neck structure utilizes multiple convolutional ConvBNReLU layers and 2D Convolutional Layer (Conv2d) operations for bounding box regression and classification, optimizing loss calculations. This structured approach ensures robust object localization and classification in medical imaging. By leveraging efficiency feature extraction and fusion mechanisms, CYOLOv8 enhances precision, computational efficiency, and real-time detection capacity in GI abnormality identification, where 1 indicates the presence of a detected GI abnormality (positive case) and 0 indicates the absence of a GI abnormality (negative case).

3.4.2 Dynamic Vortex Search (DVS)

With each repetition, the Vortex Search (VS) algorithm generates potential solutions centered on one point. In the initial iteration, the starting center (μ_0^1) is set by the problem's lower and upper limits, following iterations relocate the origin to the most ideal place identified thus far. As previously explained, this approach traps the VS method in local minimum values for different functions. This research proposes a DVS to address the previously noted drawbacks. Every single run of the DVS algorithms generates potential solutions around various centers. The DVS method's search pattern resembles a series of concurrent vortices with varying centers at every iteration. The cores of many vortexes are first identified using the VS method. Let m indicate the overall number of centers (or vortices). Assume $N_s(\mu)$ is a matrix that records the outcomes of the m centers at every iteration progress, and s is the iterative index. To determine the starting locations of these centers, use Equation (8).

$$\mu_0^1 = \mu_0^2 = \cdots = \mu_0^s = \frac{\text{upperlimit}+\text{lowerlimit}}{2}, j = 1,2,..,n \quad (8)$$

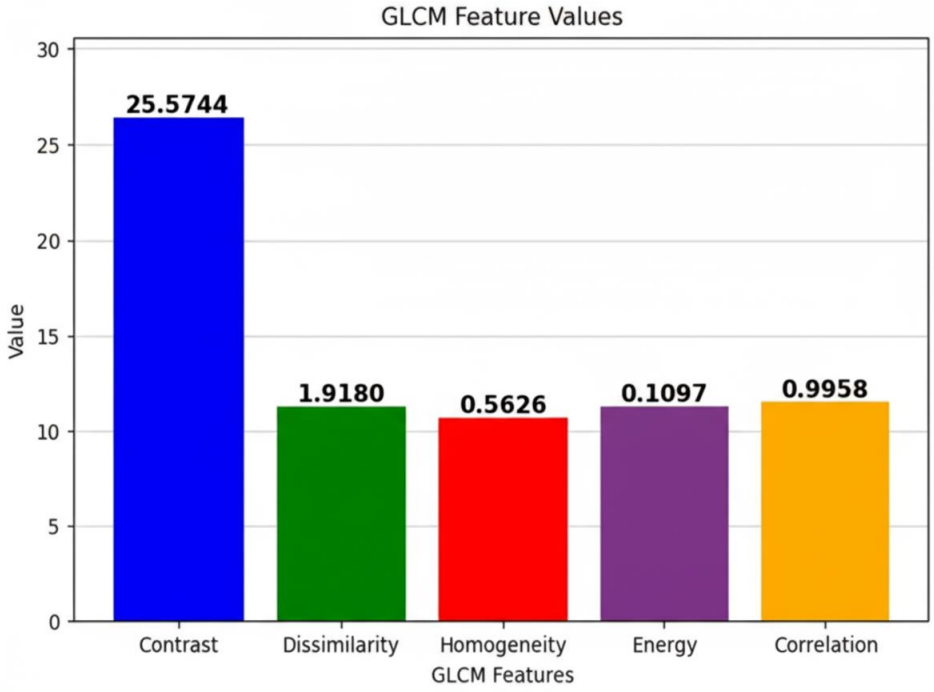

Figure 3. Graphical visualization of Feature values for GLCM.

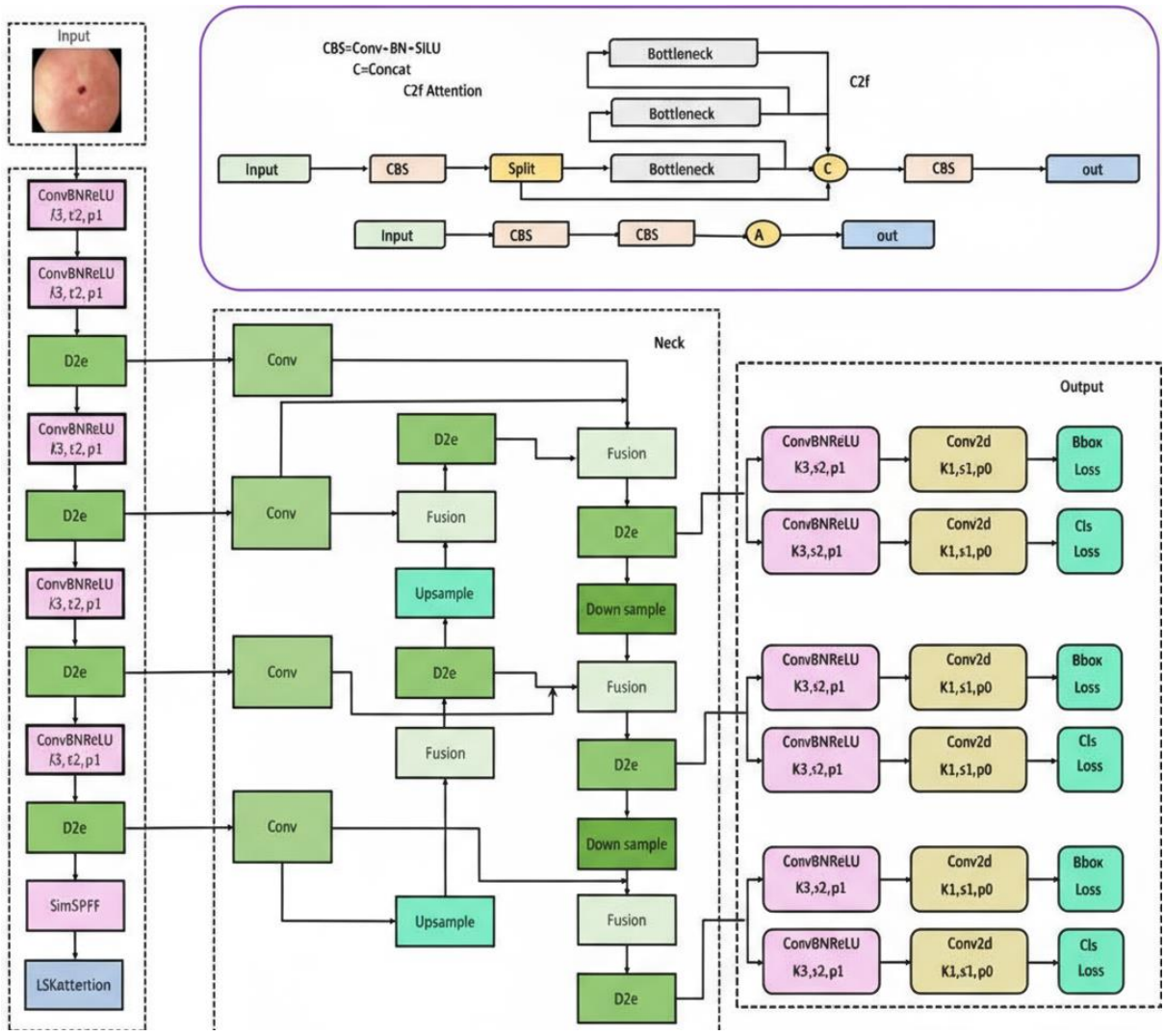

Figure 4. Structure of CYOLOv8 model **.**

Following that, the Gaussian distribution is used to produce potential solutions about the starting centers, with a beginning diameter of q_0. The total amount of potential solutions is set to$m$. However, it is worth noting that these n systems revolve around m centers. As a result, one should choose m the options surrounding every center.

$DT_s^k(t) = \{t_1, t_2, \dots, t_l\} l = 1,2, \dots, m/n$ Assume $center\ k = 2,1, \dots, n$ denotes the number of answers created during repetition s. The whole answer collection for repetition $s = 0$ could be expressed as $D_0(t) = \{D_0^1, D_0^2, .., D_0^S\}, k = 1,2, .., n$. During the selection process, for each group of approaches, an answer (that is the ideal one) $t_k \epsilon\, DT_0^k(t)$ is chosen. To do this answers that surpass the borders are moved within the confines, as shown in Equation (5). Assume that the ideal solutions for every subset are kept in a matrix $t_k \epsilon\, DT_0^k(t)$ at every iteration run. Thus, for $OBest_s(t)$ $s = 0, OBest_0(t) = \{t_1, t_2, .., t_k\}, k = 1,2, .., n$ consider that the ideal solutions in that matrix $(OBest_s(t)$ corresponds to the finest solution of every candidate answer set $D_0(t)$ s for the present repetition, that is denoted by best $Iter_{best}$. At every subsequent operation of the VS technique, the origin remains moved to the greatest solution identified thus fart_{best}. Even so, in the DVS technique, there are n centers whose coordinates require being adjusted for the following iteration. The most significant distinction between the VS and MVS algorithms emerges from this. In the MVS method, one of these points is relocated back to the greatest solutions discovered thus fart_{best}. The additional $n - 1$ centers are relocated to a new location based on the most optimal positions created around every center at repetition s and the most optimal position obtained so far, $Best_s$, as illustrated in Equation (9).

$$\mu_s^k = t_k + rand.(t_k + t_{best}) \quad (9)$$

$k = 2,1, \dots, n - 1$ and $t_k \epsilon\, OBest_{s-1}(t)$. In Equation (9), randomization is a randomly distributed arbitrary integer with $s = 1, N_1(\mu) = \{\mu_1^1, \mu_1^2, .., \mu_1^k\} k = 1,2, .., n - 1$ is calculated by utilizing the $t_k \epsilon OBest_0(t)$ locations, and the optimal location obtained so fart_{best}. The radius reduction mechanism of the MVS technique corresponds to that of the VS method. At each subsequent progress, the dimension is reduced by applying a reverse imperfect gamma operation, increasing the location of the derived solutions. This research integrates DVS optimization with a CYOLOv8 model to enhance GI abnormality detection from endoscopic imaging. The DVS-CYOLOv8 hybrid approach optimizes feature extraction, enhances localization, and improves classification accuracy while reducing computational complexity. The lightweight LSK-attention mechanism improves detection precision, while the SimSPPF module minimizes inference time. BiFPN-based multi-scale learning strengthens feature fusion, ensuring accurate object detection. The DVS algorithm enhances model hyperparameter tuning by optimizing feature selection and learning rates, reducing local minima issues.

The combination of these elements results in a strong, efficient, and scalable clarification for real-time GI abnormality classification. The working procedure of suggested DVS-CYOLOv8 model is represented in algorithm 1.

Algorithm 1. DVS-CYOLOv8

```
import numpy as np
# Initialize parameters for Dynamic Vortex Search
def initialize_dvs(pop_size, dim, lower, upper):
    return np.random.uniform(lower, upper, (pop_size, dim))
# Evaluate fitness function for each candidate solution
def evaluate_fitness(population, model):
    return np.array([model.predict(x) for x in population])
# Update Vortex Search centers dynamically
def update_vortex_centers(population, fitness):
    best_idx = np.argmin(fitness)
    best_solution = population[best_idx]
    return best_solution + np.random.normal(0, 0.1, size = best_solution.shape)
# Apply optimized hyperparameters to train Customized YOLOv8
def train_cyolov8(data, optimized_params):
    Model = CYOLOv8(optimized_params)
    model.train(data)
    return model
# Main loop for hybrid DVS-CYOLOv8
    population = initialize_dvs(pop_size = 10, dim = 5, lower = 0, upper = 1)
for iteration in range(50):
    fitness = evaluate_fitness(population, train_cyolov8)
    population = update_vortex_centers(population, fitness)
# Final model with optimized parameters
best_model = train_cyolov8(data, population[np.argmin(fitness)])
end
```

4. Experimental Findings

To enhance modeling and improve the understanding of GI abnormality detection, this research modifies the structure of the original DVS-CYOLOv8

model while maintaining its reliability. This adaptation simplifies variable complexity and computational requirements, making it suitable for scenarios where accuracy is critical and computational resources are limited. The system requirements are performed utilizing 8 GB of RAM, Intel(R) Core(TM) i5-3320M processor, CPU @ 2.60GHz, Hard disk of 200 GB in the C Drive, an OS of Windows 10 64-bit configuration, Language Tool of Python 3.13.1, Tensor Flow and Scikit-Learn, an individual edition of Anaconda https://www.anaconda.com › products › individual, and Jupyter Notebook https://jupyter.org.

The proposed DVS-CYOLOv8 model was applied to the data to classify four key GI conditions: Normal-Pylorus, Polyps, Ulcerative Colitis, and Esophagitis. The confusion matrix (Figure 5) illustrates the categorization efficiency of the proposed model. High classification accuracy is observed, particularly for Esophagitis (74 correctly classified instances) and Ulcerative Colitis (67 correctly classified instances), indicating the model's effectiveness in identifying these abnormalities. Normal-Pylorus has 60 correct predictions, but misclassifications (6 as Polyps, 8 as Ulcerative Colitis, and 1 as Esophagitis) suggest some overlap in visual features between conditions. Polyps are categorized correctly in 66 cases but in few misclassifications that turn out to be in other categories. Based on the overall classification performance, it is clear that DVS-CYOLOv8 is effective in detecting and classifying GI abnormalities with some allowance that was made concerning visually similar conditions. These findings indicate the efficiency of DVS-CYOLOv8 in real-time endoscopic diagnostics, decreasing the volume of work and enhancing uniformity of the diagnosis of GI diseases.

Receiver Operating Characteristic (ROC) curve (Figure 6) assesses the level of performance of the proposed DVS-CYOLOv8 model in the detection of Normal-Pylorus, Polyps, Ulcerative Colitis, and Esophagitis in the Kvasir Dataset. The AUC values are between 0.97 and 0.99 which equate to a high percentage of accuracy in classification. Esophagitis (Class 3) records the greatest AUC (0.99), which indicates effective model performance in differentiating this one. Classes 0 (Normal-Pylorus) and 2 (Ulcerative Colitis) have AUC = 0.98 demonstrating an excellent discrimination between these classes. Class 1 (Polyps) shows the poorest AUC (0.97), and therefore it contains a few false positives in relation to other classes. The high AUC values indicate that DVS-CYOLOv8 would be very good at the detection of GI abnormalities, minimizing false-positives by retaining the high true-positive value. This shows that the proposed model can be successfully used to perform precise automated endoscopic image analysis, and, as a result, provide early identification and clinical decision-making.

The ROC curve (Figure 7) measures the overall fitness of the general L community of the DVS-CYOLOv8 model in the Kvasir dataset in classifying Normal-Pylorus, Polyps, Ulcerative Colitis, and Esophagitis. AUC is 0.98 based on which the correctness of the categorization is ranked as excellent. The curve is near the upper-left point meaning that the model is efficient in discrimination between various GI abnormalities. The accuracy (AUC=0.98) further indicates that DVS-CYOLOv8 has very high sensitivity and specificity with minimal types of misclassification. This highlights the possibility of the model in automating the endoscopic image analysis to identify the early-stage disease and diagnosis process.

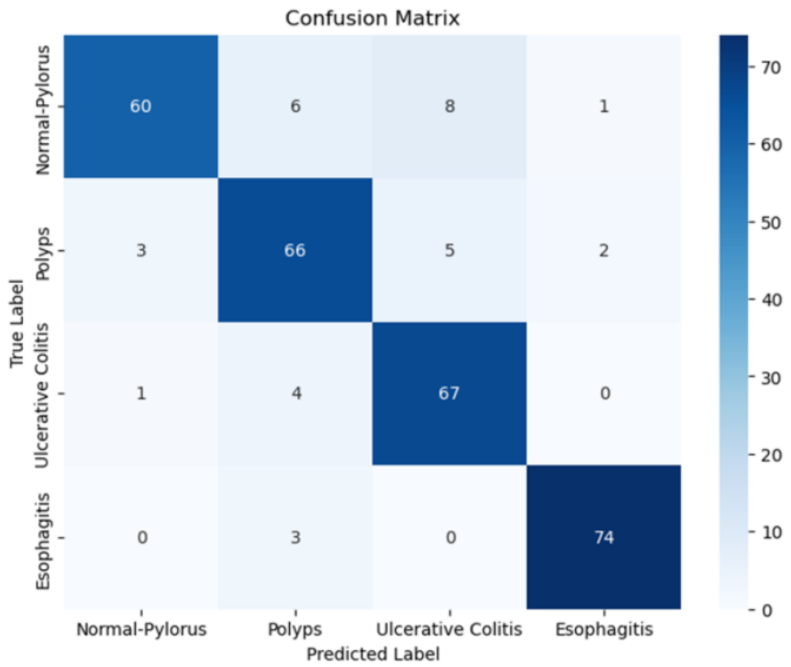

Figure 5. Confusion Matrix of DVS-CYOLOv8 model

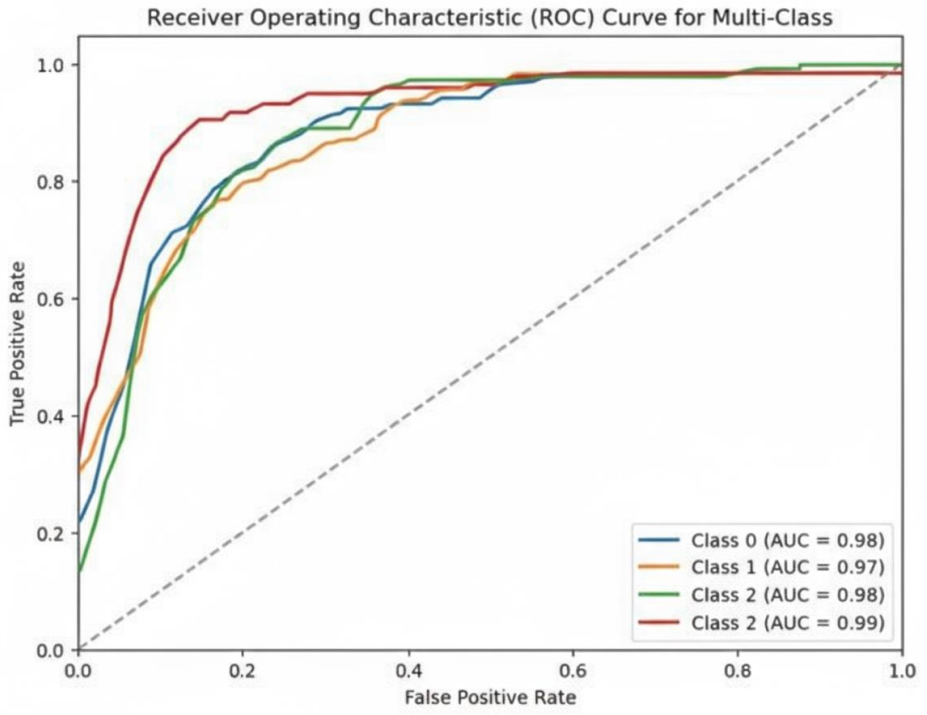

Figure 6. ROC Curve for Multi-Class data

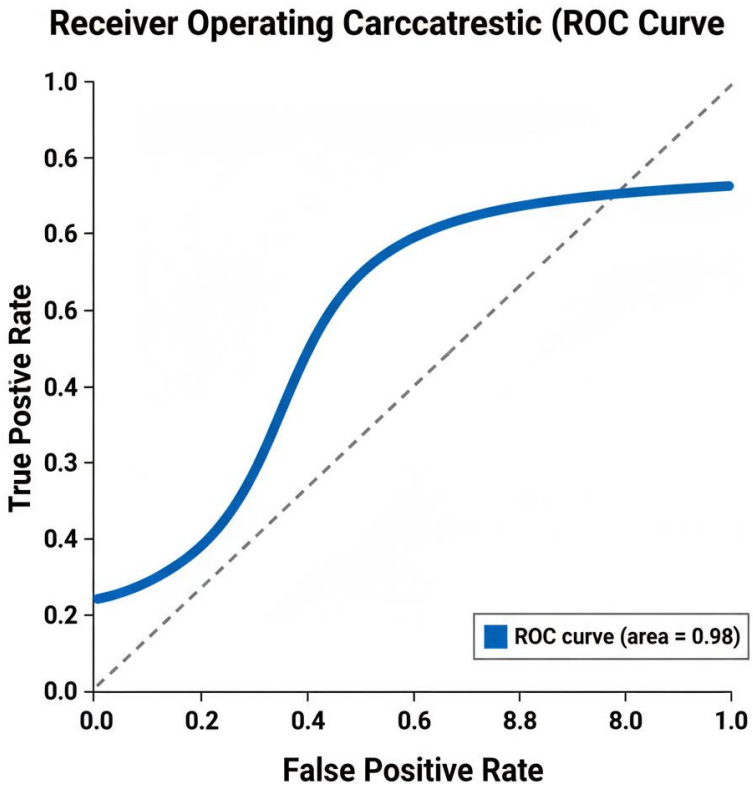

Figure 7. Graphical representation of Roc Curve

4.1 Comparison Analysis

Accuracy determines the accuracy of a method by evaluating the proportion of properly classified instances out of total predictions (Table 2 and Figure 8). A higher accuracy indicates better generalization and reliability in detecting GI abnormalities. The proposed DVS-CYOLOv8 achieves the highest accuracy of 99.11%, surpassing the Modified Salp Swarm Algorithm with Deep Learning Gastrointestinal Tract Disease Classification (MSSADL-GITDC) (98.03%) and Bayesian Optimized Support Vector Machine (SVM) (97.0%), while traditional methods like Bayesian (88.34%) perform significantly lower. This result demonstrates that DVS-CYOLOv8 can efficiently identify abnormalities across various endoscopic conditions with minimal misclassification, ensuring reliable detection for real-world clinical applications. Precision evaluates the method's capability to properly recognize positive cases (abnormalities) while decreasing false positives.

Table 2. Comparison methods across several metrics

Methods	Accuracy (%)	Precision (%)	Recall (%)
Equations	$Accuracy \frac{TP+TN}{TP+TN+FP+FN}$	$Precision \frac{TP}{TP+TF}$	$Recall = \frac{TP}{TF+TN}$
Softmax (Nouman Noor et al., 2023)	94.68	96.94	93.22
Bayesian (Nouman Noor et al., 2023)	88.34	91.64	88.35
MSSADL-GITDC (Obayya et al., 2023)	98.03	92.16	92.13
LR Tree (Obayya et al., 2023)	94.13	87.04	89.17
Bayesian Optimized SVM (Saeed et al., 2022)	97.0	96.9	96.9
Medium KNN (Saeed et al., 2022)	94.1	94.2	94.1
DVS-CYOLOv8 (Proposed)	99.11	98.24	98.18

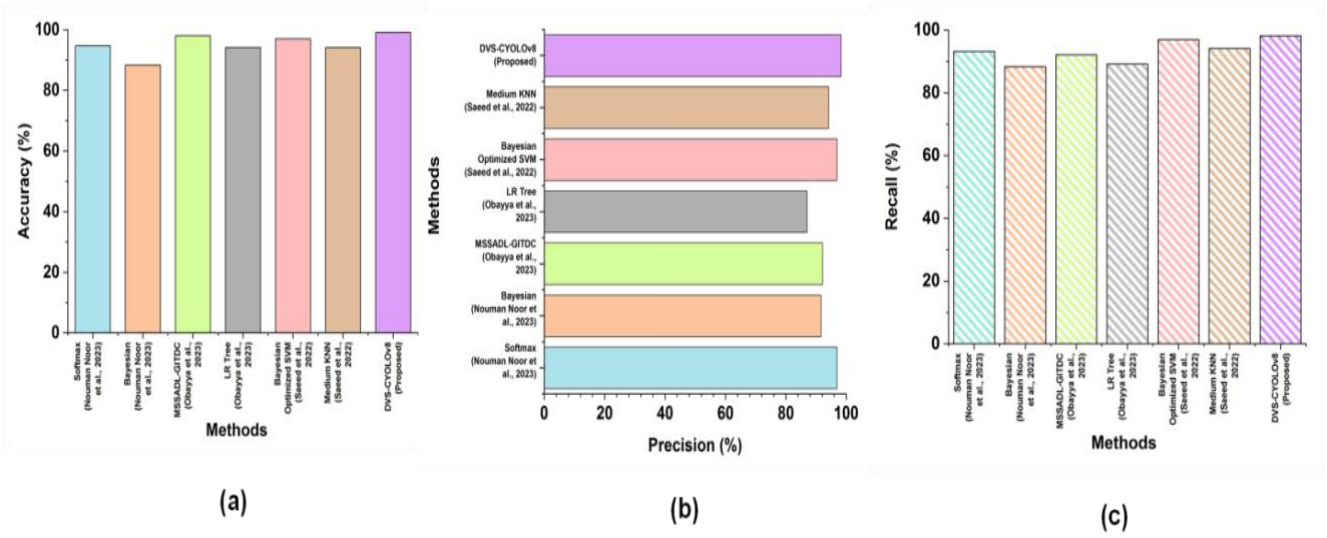

Figure 8. Comparison methods across several metrics

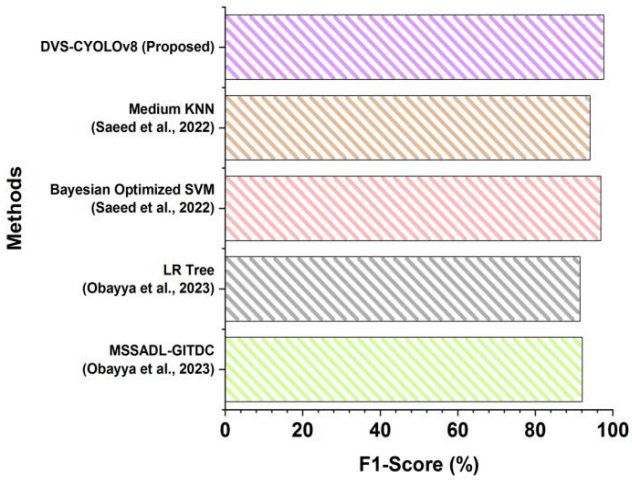

Figure 9. Comparison methods across F1-score

Table 3. Comparison methods across F1-score

Methods	F1-Score (%)
Equation	$F1-Score = \frac{2TP}{2TP+FP+FN}$
MSSADL-GITDC (Obayya *et al.,* 2023)	92.11
LR Tree (Obayya *et al.,* 2023)	91.53
Bayesian Optimized SVM (Saeed *et al.,* 2022)	96.9
Medium KNN (Saeed *et al.*, 2022)	94.1
DVS-CYOLOv8 (Proposed)	97.66

A high precision score indicates that most predicted abnormalities are indeed correct. DVS-CYOLOv8 attains 98.24% precision, outperforming Bayesian Optimized SVM (96.9%) and significantly exceeding Logistic Regression (LR) Tree (87.04%), which shows a higher rate of false positives. This finding shows that the proposed model will minimize the number of errors on misdiagnosis and this is important since in medical imaging unwarranted intervention or patient anxiety can be avoided. Recall is the proportion of abnormalities actually identified through the specified amount of abnormalities that the method identifies, focusing on the ability of the method to find subtle lesions. The DVS-CYOLOv8 reaches better recall of 98.18%, compared to the MSSADL-GITDC (92.13%) and Bayesian (88.35%) that miss some abnormalities. This finding shows that the suggested model allows broadly identifying GI abnormalities, lowering the risk of lacking essential abnormalities and enhancing good diagnostic reliability.

The F1-score is a balanced metric to give a very comprehensive assessment of the method's effectiveness. The higher the F1-score, the stronger the balance between proper detections and reduced misclassification. DVS-CYOLOv8 scores 97.66%, the highest among all methods, followed by Bayesian Optimized SVM (96.9%) and MSSADL-GITDC (92.11%) (Table 3 and Figure 9). This reveals that the model in question achieves an adequate balance between the promotion of sensitivity and the firm stand on specificity, which will make it a decent candidate for real-time endoscopic abnormality diagnosis with minimal errors.

5. Discussion

Existing methods for classification of GI tract diseases exhibit considerable drawbacks. Softmax by Nouman Noor [32] has poor generalization. It becomes overconfident when classifying things incorrectly. Bayesian approaches face issues with their computational complexity and slow inference speed. When applied in high-dimensional situations, the MSAL-GITDC technique is not as resilient as other methods [33] LR tree cannot work against non-linear objects, switching to non-efficient feature extraction . SVM optimized by Bayesian , on the contrary, was heavy in computation even if it got optimized parameters. However, when it comes to working on large datasets, medium K-Nearest Neighbor (KNN) [34] does not really perform well since it has a distance metric concept to rely on and therefore takes longer with displayed memory. When compared with existing methods, the proposed DVS-CYOLOv8 achieves significant improvements. Softmax, while simple, fails to generalize well and often exhibits overconfidence, whereas DVS-CYOLOv8 ensures reliable probabilistic predictions with reduced misclassifications. Bayesian and SVM-based methods are computationally heavy, limiting real-time usability, but the proposed model delivers faster inference through its efficient region proposal mechanism.

The suggested Dynamic Vortex Search-tuned Customized YOLOv8 (DVS-CYOLOv8) model is shown to be extremely promising and first-order in the detection and classification of GI abnormalities on endoscopic imaging. Conventional CADe system is likely to have difficulty in achieving high sensitivity with timely sensitivity in real time. These difficulties are related to the weak visual specifics of early-stage abnormalities, the inconsistency of their morphology, and overbalancing the classes of annotated datasets. The DVS-CYOLOv8 method is a good approach to mitigate such limitations directly by considering proper preprocessing methods, effective feature sufficing, and efficient hyper parameter optimization.

A crucial element of the performance improvement is the original contribution of Dynamic Vortex Search optimizer, which automatically optimizes key hyper parameters including anchor box sizes, confidence thresholds and non-maximum suppression rates. Unlike manual or heuristic optimization schemes, the search parameters of the DVS evolve dynamically, equally allowing the network to concretize on clinically meaningful regions of interest and inhibit counter-productive background noise. This leads to fewer false positives, better lesion localization and a better reliability

across datasets that are heterogeneous. The results demonstrated with the accuracy of 99.11 percent, precision of 98.24 percent, recall of 98.18 percent, and F1-score of 97.66 percent underscore the superiority of the method over the traditional detection architectures and standalone variants of YOLO. Precision-recall balance is of particular concern in clinical settings where false positives and underdiagnoses may result in deploying interventions that are unnecessary and false negatives may cause a delay in critical treatment outcomes. The abnormally high F1-score implies that DVS-CYOLOv8 attains an advantaged trade-off and thus provides a consistent diagnostic suitability.

Multi scale segmentation of CYOLOv8 also enhances the robustness of the method. Various GI abnormalities present as very low level irregularities e.g., tiny polyps or microscopic ulcerative spots that are often missed during feature extraction in traditional models, since down-sampling reduces the level of aberrations. With the multi-scale feature representation, not only is the macro but also the micro-scale structures captured, and this brings about the proper representation of boundaries and thus increased generalization. The inclusion of gradient-based texture and boundary descriptors helpful in improving abnormality differentiation against normal mucosal patterns that tend to be obscured by uneven light in endoscopy is also due to such preprocessing.

LR Tree and MSAL-GITDC approaches lack robustness in handling non-linear and high-dimensional data, whereas DVS-CYOLOv8 leverages advanced multi-scale contextual learning to extract richer features and maintain robustness across diverse clinical scenarios. KNN struggles with scalability and memory inefficiency in large datasets, while the proposed framework significantly lowers computational complexity without compromising accuracy. Collectively, these comparisons establish that DVS-CYOLOv8 surpasses traditional and recent techniques by achieving a balance of computational efficiency, scalability, and diagnostic precision, making it better suited for clinical adoption. The proposed DVS-CYOLOv8 model overcomes aforementioned drawbacks by merging deep vision segmentation DVS framework with optimized YOLOv8 architecture. The feature extraction was enhanced by better contextual learning across multiple scales, thereby improving classification performance. Furthermore, non-linear relationships are efficiently handled, commonly by Bayesian and LR Tree, but with computational efficiency. It ensures near-exemplary robustness in high-dimensional image analysis compared to the MSSADL-GITDC. The model alleviates this concern compared with Medium KNN by reducing the computational complexity through highly efficient region proposal mechanisms. Collectively, the research work alarms that DVS-CYOLOv8 attains an elevation in the diagnostic accuracy, faster inference speed, and eventually better generalization for GI disease classification. Experimental results show high improvements in proving their efficacy in real-world clinical applications.

6. Conclusion

GI abnormalities detected through endoscopic imaging are vital for early diagnosis and treatment planning. Nevertheless, accurate classification is a complex challenge offered by endoscopic images due to their variability, and more sophisticated DL techniques are nowadays applied to ensure a precise outcome. In this research, a DVS-CYOLOv8 model is proposed to effectively improve the classification of GI-related diseases through enhanced feature extraction, multi-scale contextual learning, and efficient region proposal mechanism. The method offers fairness and improved computational efficiency and generalization to medical image analysis compared with the classical methodologies.

Results display that DVS-CYOLOv8 achieves a classification accuracy of 99.11%, F1-score of 97.66%, precision of 98.24%, and recall of 98.18% outperforming existing state-of-the-art models in GI abnormality detection. Additionally, the model significantly reduces false positives and enhances real-time processing efficiency, making it highly effective for clinical applications. The research has limitations since it is based on high-quality labeled datasets for training DL models, which in turn demand numerous computational resources. In addition, performance validation across various datasets and real-world clinical settings requires further investigation.

Further research should also incorporate the principles of self-supervised learning to enhance method performance using limited labeled samples. The DVS-CYOLOv8 model depends heavily on high-quality annotated datasets, which are costly and scarce in medical imaging. Its training demands significant computational resources, limiting deployment in low-resource hospitals. Dataset variability across demographics and imaging devices may introduce bias, while the black-box nature of deep learning restricts interpretability. Ethical, privacy, and regulatory constraints further challenge large-scale clinical adoption. Future research should focus on self-supervised learning to minimize labeled data requirements and explore multi-modal imaging for richer diagnostic insights. Explainable AI can enhance interpretability and clinical trust. Lightweight optimization for edge devices which support real-time deployment. Federated learning offers privacy-preserving collaboration, while validation across diverse clinical settings ensures generalization, fostering robust, ethical, and widely adoptable AI-based diagnosis. Moreover, multi-modal medical imaging and explainable AI techniques can be integrated to improve model interpretability and clinical acceptance, thereby

providing better foundations for reliable and intelligent GI disease diagnosis.

References

[1] M.L. Zhang, A. Neyaz, D. Patil, J. Chen, M. Dougan, V. Deshpande, Immune-related adverse events in the GI tract: diagnostic utility of upper GI biopsies. Histopathology, 76(2), (2020) 233−243. https://doi.org/10.1111/his.13963

[2] S. Nazarian, I. Gkouzionis, M. Kawka, M. Jamroziak, J. Lloyd, A. Darzi, N. Patel, D.S. Elson, C.J. Peters, Real-time tracking and classification of tumor and nontumor tissue in upper GI cancers using diffuse reflectance spectroscopy for resection margin assessment. JAMA surgery, 157(11), (2022) e223899−e223899. https://doi.org/10.1001/jamasurg.2022.3899

[3] R. Nudel, V. Appadurai, A.J. Schork, A. Buil, J. Bybjerg-Grauholm, A.D. Børglum, M.J. Daly, O. Mors, D.M. Hougaard, P.B. Mortensen, T. Werge, A large population-based investigation into the genetics of susceptibility to GI infections and the link between GI infections and mental illness. Human genetics, 139, (2020) 593−604. https://doi.org/10.1007/s00439-020-02140-8

[4] A.R. Blaser, M. Padar, M. Mändul, M. Elke, G. Engel, C. Fischer, K. Giabicani, M. Gold, T. Hess, B. Hiesmayr, M. Jakob, S.M., Development of the GI dysfunction score (GIDS) for critically ill patients–A prospective multicenter observational study (iSOFA study). Clinical Nutrition, 40(8), (2021) 4932−4940. https://doi.org/10.1016/j.clnu.2021.07.015

[5] C.Y. Lam, O.S. Palsson, W.E. Whitehead, A.D. Sperber, H. Tornblom, M. Simren, I. Aziz, Rome IV functional GI disorders and health impairment in subjects with hypermobility spectrum disorders or hypermobile Ehlers-Danlos syndrome. Clinical Gastroenterology and Hepatology, 19(2), (2021) 277−287. https://doi.org/10.1016/j.cgh.2020.02.034

[6] J. Lasekan, Y. Choe, S. Dvoretskiy, A. Devitt, S. Zhang, A. Mackey, K. Wulf, R. Buck, C. Steele, M. Johnson, G. Baggs, Growth and GI tolerance in healthy term infants fed milk-based infant formula supplemented with five human milk oligosaccharides (HMOs): A randomized multicenter trial. Nutrients, 14(13), (2022) 2625. https://doi.org/10.3390/nu14132625

[7] T. Chaemsupaphan, J. Limsrivilai, C. Thongdee, A. Sudcharoen, A. Pongpaibul, N. Pausawasdi, P. Charatcharoenwitthaya, Patient characteristics, clinical manifestations, prognosis, and factors associated with GI cytomegalovirus infection in immunocompetent patients. BMC gastroenterology, 20, (2020) 1−12. https://doi.org/10.1186/s12876-020-1174-y

[8] R. Agarwala, S.S. Rana, R. Sharma, M. Kang, U. Gorsi, R. Gupta, GI failure is a predictor of poor outcome in patients with acute pancreatitis. Digestive Diseases and Sciences, 65, (2020) 2419−2426. https://doi.org/10.1007/s10620-019-05952-5

[9] R.S.E.E. Hassan, S.O.S. Osman, M.A.S. Aabdeen, W.E.A. Mohamed, R.S.E.E. Hassan, S.O.O. Mohamed, Incidence and root causes of surgical site infections after GI surgery at a public teaching hospital in Sudan. Patient Safety in Surgery, 14, (2020) 1−7. https://doi.org/10.1186/s13037-020-00272-4

[10] N. El Koofy, H.M.N. Eldin, W. Mohamed, M. Gad, S. Tarek, G. El Tagy, Impact of preoperative nutritional status on surgical outcomes in patients with pediatric GI surgery. Clinical and experimental pediatrics, 64(9), (2020) 473. https://doi.org/10.3345/cep.2020.00458

[11] G. Vanella, G. Capurso, C. Burti, L. Fanti, L. Ricciardiello, A.S. Lino, I. Boskoski, M. Bronswijk, A. Tyberg, G.K.K. Nair, S. Angeletti, GI mucosal damage in patients with COVID-19 undergoing endoscopy: an international multicentre study. BMJ open gastroenterology, 8(1), (2021) e000578. https://doi.org/10.1136/bmjgast-2020-000578

[12] F.W.D. Tai, O.S. Palsson, C.Y. Lam, W.E. Whitehead, A.D. Sperber, H. Tornblom, M. Simren, I. Aziz, Functional GI disorders are increased in joint hypermobility-related disorders with concomitant postural orthostatic tachycardia syndrome. Neurogastroenterology & Motility, 32(12), (2020) e13975. https://doi.org/10.1111/nmo.13975

[13] I. Iqbal, K. Walayat, M.U. Kakar, J. Ma, Automated identification of human GI tract abnormalities based on a deep convolutional neural network with endoscopic images. Intelligent Systems with Applications, 16, (2022) 200149. https://doi.org/10.1016/j.iswa.2022.200149

[14] J.Y. Park, Image-enhanced endoscopy in upper GI disease: focusing on texture and color enhancement imaging and red dichromatic imaging. Clinical endoscopy, (2024). https://doi.org/10.5946/ce.2024.159

[15] M.A. Berbís, J. Aneiros-Fernández, F.J.M. Olivares, E. Nava, A. Luna, Role of AI in multidisciplinary imaging diagnosis of GI diseases. World Journal of gastroenterology, 27(27), (2021) 4395. https://dx.doi.org/10.3748/wjg.v27.i27.4395

[16] A. Sharma, R. Kumar, P. Garg, DL-based prediction model for diagnosing GI diseases

using endoscopy images. International Journal of Medical Informatics, 177, (2023) 105142. https://doi.org/10.1016/j.ijmedinf.2023.105142

[17] Q. He, S. Bano, O.F. Ahmad, B. Yang, X. Chen, P. Valdastri, L.B. Lovat, D. Stoyanov, S. Zuo, DL-based anatomical site classification for upper GI endoscopy. International journal of computer assisted radiol ogy and surgery, 15, (2020) 1085−1094. https://doi.org/10.1007/s11548-020-02148-5

[18] H. Yu, R. Singh, S.H. Shin, K.Y. Ho, AI in upper GI endoscopy-current status, challenges and future promise. Journal of Gastroenterology and Hepatology, 36(1), (2021) 20−24. https://doi.org/10.1111/jgh.15354

[19] J. Wu, J. Chen, J. Cai, Application of AI in GI endoscopy.Journal of Clinical Gastroenterology , 55(2), (2021) 110−120. https://journals.lww.com/jcge/toc/2021/02000

[20] M.N. Noor, M. Nazir, I. Ashraf, N.A. Almujally, M. Aslam, S. Fizzah Jilani, GastroNet: A robust attention-based DL and cosine similarity feature selection framework for GI disease classification from endoscopic images. CAAI Transactions on Intelligence Technology, (2023). https://doi.org/10.1049/cit2.12231

[21] J. Yogapriya, V. Chandran, M.G. Sumithra, P. Anitha, P. Jenopaul, C. Suresh Gnana Dhas, GI tract disease classification from wireless endoscopy images using pretrained DL model. Computational and mathematical methods in m edicine, 2021(1), (2021) 5940433. https://doi.org/10.1155/2021/5940433

[22] R. Pannala, K. Krishnan, J. Melson, M.A. Parsi, A.R. Schulman, S. Sullivan, G. Trikudanathan, A.J. Trindade, R.R. Watson, J.T. Maple, D.R. Lichtenstein, AI in GI endoscopy. VideoGIE, 5(12), (2020) 598−613. https://doi.org/10.1016/j.vgie.2020.08.013

[23] K. Ramamurthy, T.T. George, Y. Shah, P. Sasidhar, A novel multi-feature fusion method for classification of GI diseases using endoscopy images. Diagnostics, 12(10), (2022) 2316. https://doi.org/10.3390/diagnostics12102316

[24] S. Wang, Y. Cong, H. Zhu, X. Chen, L. Qu, H. Fan, Q. Zhang, M. Liu, Multi-scale context-guided deep network for automated lesion segmentation with endoscopy images of GI tract. IEEE Jour, (2020). https://doi.org/10.1109/JBHI.2020.2997760

[25] D.H. Ballard, N. Wake, J. Witowski, F.J. Rybicki, A. Sheikh, Radiological Society of North America (RSNA) 3D Printing Special Interest Group (SIG) clinical situations for which 3D printing is considered an appropriate representation or extension of data contained in a medical imaging examination: abdominal, hepatobiliary, and GI conditions. 3D printing in medicine, 6, (2020) 1−7. https://doi.org/10.1186/s41205-020-00065-6

[26] M. Owais, M. Arsalan, T. Mahmood, J.K. Kang, K.R. Park, Automated diagnosis of various GI lesions using a DL–based classification and retrieval framework with a large endoscopic database: model development and validation. Journal of medical Internet research, 22(11), (2020) e18563. https://doi.org/10.2196/18563

[27] S. Tang, X. Yu, C.F. Cheang, Y. Liang, P. Zhao, H.H. Yu, I.C. Choi, Transformer-based multi-task learning for classification and segmentation of GI tract endoscopic images. Computers in biology and medicine, 157, (2023) 106723. https://doi.org/10.1016/j.compbiomed.2023.106723

[28] Z. Xiao, J. Lu, X. Wang, N. Li, Y. Wang, N. Zhao, WCE-DCGAN: A data augmentation method based on wireless capsule endoscopy images for GI disease detection. IET Image Processing, 17(4), (2023) 1170−1180. https://doi.org/10.1049/ipr2.12704

[29] M. Hmoud Al-Adhaileh, E. Mohammed Senan, F.W. Alsaade, T.H.H. Aldhyani, N. Alsharif, A. Abdullah Alqarni, M.I. Uddin, M.Y. Alzahrani, E.D. Alzain, M.E. Jadhav, DL algorithms for detection and classification of GI diseases. Complexity, 2021(1), (2021) 6170416. https://doi.org/10.1155/2021/6170416

[30] V. Raut, R. Gunjan, V.V. Shete, U.D. Eknath, GI tract disease segmentation and classification in wireless capsule endoscopy using intelligent DL model. Computer Methods in Biomechanics and Biom edical Engineering: Imaging & Visualization, 11(3), (2023) 606−622. https://doi.org/10.1080/21681163.2022.2099298

[31] https://www.kaggle.com/datasets/abdallahwagih/kvasir-dataset-for-classification-and-segmentation

[32] M. Nouman Noor, M. Nazir, S.A. Khan, I. Ashraf, O.Y. Song, Localization and classification of GI tract disorders using explainable AI from endoscopic images. Applied Sciences, 13(15), (2023) 9031. https://doi.org/10.3390/app13159031

[33] M. Obayya, F.N. Al-Wesabi, M. Maashi, A. Mohamed, M.A. Hamza, S. Drar, I. Yaseen, M.I. Alsaid, Modified salp swarm algorithm with DL based GI tract disease classification on endoscopic images. Ieee Access, 11, (2023) 25959−25967. https://doi.org/10.1109/ACCESS.2023.3256084

[34] T. Saeed, C. Kiong Loo, M.S. Safiruz Kassim, Ensembles of DL framework for stomach

abnormalities classification. Computers, Materials & Continua, 70(3), (2022). https://doi.org/10.32604/cmc.2022.019076

Authors Contribution Statement

Both authors equally contributed to this work, read and approved the final version of the manuscript.

Funding

The authors declare that no funds, grants or any other support were received during the preparation of this manuscript.

Competing Interests

The authors declare that there are no conflicts of interest regarding the publication of this manuscript.

Data Availability

The data supporting the findings of this study can be obtained from the corresponding author upon reasonable request.

Has this article screened for similarity?

Yes

About the License